Ballasted & electrically steerable carbon nanotube field emitters

M. T. Cole[*,a,b], C. Li[a,c], K. Qu[c], Y. Zhang[a], B. Wang[c], D. Pribat[d] & W. I. Milne[a,e]

[a] Dept. of Engineering, Electrical Engineering Division, University of Cambridge, 9 JJ Thomson Avenue, CB3 0FA, Cambridge, United Kingdom; [b] AIXTRON Ltd., Swavesey, CB24 4FQ, Cambridge, United Kingdom; [c] Display Research Centre, School of Electronic Science & Engineering, Southeast University, Nanjing, 210096, People's Republic of China; [d] Dept. of Energy Science, Sungkyunkwan University, Suwon, 440746, Republic of Korea; [e] Dept. of Information Display, Kyung Hee University, Seoul 130701, Republic of Korea.

ABSTRACT

Here we present our on-going efforts toward the development of stable ballasted carbon nanotube-based field emitters employing hydrothermally synthesized zinc oxide nanowires and thin film silicon-on-insulator substrates. The semiconducting channel in each controllably limits the emission current thereby preventing detrimental burn-out of individual emitters that occurs due to unavoidable statistical variability in emitter characteristics, particularly in their length. Fabrication details and emitter characterization are discussed in addition to their field emission performance. The development of a beam steerable triode electron emitter formed from hexagonal carbon nanotube arrays with central focusing nanotube electrodes, is also described. Numerical *ab-initio* simulations are presented to account for the empirical emission characteristics. Our engineered ballasted emitters have shown some of the lowest reported lifetime variations (< 0.7%) with on-times of < 1 ms, making them ideally-suited for next-generation displays, environmental lighting and portable x-rays sources.

Keywords: carbon nanotubes, field emission, ballasted, zinc oxide nanowires, SOI, triode

1. INTRODUCTION

Carbon, a semi-metallic element that forms many novel low-dimensional allotropes, is critical in a wide range of cold-cathode field emission electron source applications including light-weight flexible and transparent flat panel displays[4,5,6] portable x-ray generators[7, 8], electron beam and nano-lithography systems[9, 10], travelling wave tubes[11], and microwave amplifiers[12]. Suitable materials that offer the whisker-like geometries necessary for high current densities, crystallographically stable, low-extraction electric fields, increased pressure functionality, low weight, and high lifetimes; are hitherto lacking. Carbon nanotubes (CNTs) offer one such solution. These high-aspect ratio, one-dimensional, low axial resistance nanoscale wires formed from concentrically nested sp^2-bonded graphene planes are ideally suited for field emission applications. They are chemically robust and their emission characteristics are highly resistant to variations in incident radiation and temperature[13]. CNTs have a near-instantaneous[3] response to applied electric fields and offer high current carrying capabilities and significant resistance to electromigration.

Though CNTs have repeatedly shown impressive field emission performance, such as high emission current densities and low turn-on electric fields[8, 14-22] they are plagued by burn-out issues. CNT burn-out – the removal of individual CNTs due to the over-emission of current inducing Joule-heating and subsequent structural deformation and eventual removal - is exacerbated by the use of screen printed CNT pastes which form spaghetti-like mats of varied height. Variation in emitter height is repeatedly implicated as being the dominate mechanism instigating burn-off[23, 24]. In contrast, engineered vertically aligned arrays of CNTs offer high current densities and beam alignment. However, some

Carbon Nanotubes, Graphene, and Associated Devices V, edited by Didier Pribat, Young-Hee Lee, Manijeh Razeghi,
Proc. of SPIE Vol. 8462, 84620R · © 2012 SPIE · CCC code: 0277-786/12/$18 · doi: 10.1117/12.932388

non-uniformity in emitter height still exists which degrades the device lifetime dramatically. Thus the electron-extracting local electric field at the apex of the longest CNTs dominates resulting in a small proportion of the available CNT population emitting the majority of the measurable current and burning-off. Over time, and cycling of the extraction bias, these dominating CNTs emit increasingly high current densities, which (in the case of CNT as the resistance decreases sub-linearly with temperature) stimulates further current emission. This avalanche in the emission current halts when the crystalline structure of the CNTs thermally degrades, and the CNTs burn-off. Stable, long-lasting emitters are necessary for commercially viable electron sources. Thus, it is critical to ensure all the emitters liberate near-equivalent current densities consistently, at nominally equivalent conditions. One way to achieve increased lifetimes is *via* the integration of protection hardware such as ballast, current-limiting resistances.

1.1 Ballasted Emission – Zinc Oxide Nanowires (ZnO NWs)

The value of the integrated ballast resistances must be comparable in size to the differentiated field emission I-V characteristics. Such large resistances are difficult to realize using metallic thin films deposited by traditional PVD techniques. However, Zinc oxide (ZnO) - an *n*-type wide band gap, low-carrier density, indirect compound semiconductor - offers one viable solution. In addition to large exciton binding energy, the thermal stability and high oxidation resistance, compared to nanotubes[25], make semiconducting oxide nanostructures particularly appealing in 'poor' vacuum field emission applications[26]. Another important benefit offered by ZnO NWs in particular is that their morphology readily adopts sharp nanowire-like forms that are well-suited to field emission applications. These whisker-like emitters can conformally coat arbitrary surfaces, producing mechanically flexible thin films grown *via* facile, inexpensive polymer-compatible low-temperature hydrothermal techniques[27].

Figure 1a and **1b** show SEM micrographs of a PET-supported, chemically untreated, dry-transferred multi-walled carbon nanotube (MWCNT) thin film[2] coated with ZnO NWs. The inset of **Figure 1a** shows a patterned thin film MWCNT emitter achieved by combining standard low-cost laser jet printing with a catalyst passivation process prior to CVD. Dry-transferred (rolled) MWCNT films were typically ~20 μm thick. HR-TEM analysis indicated the high graphitic quality of the MWCNTs which had between 2 and 5 walls, are approximately 500 μm in length and were 25±10 nm in diameter. Vertically aligned ZnO NWs were grown by immersion coating the PET/MWCNT substrates in an equimolar solution of DI water, 25 mM zinc nitrate hexahydrate ($Zn(NO3)2•6H2O$, Sigma Aldrich) and hexamethylenetetramine (HMTA, Sigma Aldrich) heated to 80°C for up to 4 h. Areal SEM micrographs of a rolled MWCNT film and a MWCNT film with a ZnO NW coating are given in **Figure 1a** and **1b**, respectively. The ZnO NWs were 4 μm long, 63±11 nm in diameter and had an approximate packing density of $5x10^5$ cm^{-2}. The crystallinity of the hydrothermally grown ZnO NWs was studied *in-situ* and by drop cast IPA dispersions on Si<100> and analyzed by X-ray diffractometry (XRD, Bruker D8, Cu-Kα radiation, theta-theta geometry at 1.541 Å). The ZnO NWs were highly crystalline with assigned unit cell lattice parameters of a = 3.25 Å and c = 5.21 Å. An hexagonal wurtzite structure similar to bulk ZnO was noted. Strong 2θ=26° peaks originate from the MWCNTs composite graphitic planes. HR-TEM and select-area electron diffraction pattern (JEOL 2000FX TEM operated at 400 keV) verify the high crystallinity inferred from XRD. EDX clearly indicates both purity and stoichiometry. Transmission optical spectrophotometry suggests a Tauc gap of 3.37 eV, identical to the value for bulk ZnO[28].

The emission current and Fowler-Nordheim characteristics of the pristine MWCNT and ZnO NW+MWCNT films are shown in **Figure 2c** and **2d.** Assuming work functions of 5.3 eV (ZnO) and 5.0 eV (MWCNTs)[29], the average field enhancement factors of the pristine MWCNTs and ZnO NW coated MWCNTs were 3500 and 3200, respectively. Field screening, associated with dense NW packing, most likely reduced the enhancement factor in this latter case. Surface protrusions, such as individual nanotubes and nanotube bundles, with large enhancement factors emit at lower fields. As the extraction field increases these dominating nanotubes emit ever increasing current densities and eventually burn out before other emitters reach their threshold field. Thus, the global current density is limited by the number of active emitters. However, the axial resistivity of the ZnO NWs limits the emission current from the dominating nanotube emitters. Thus, these emitters do not burn out prior to the activation of other, less-preferential, emitters. The effect of the ballast resistance can be clearly seen in the FN plot shown in **Figure 1d**. The maximum emission current is reduced by

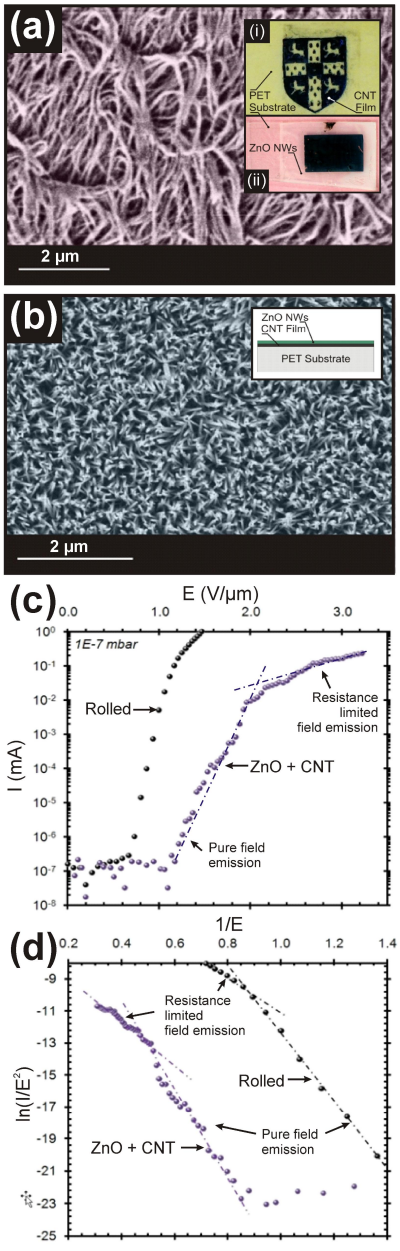

Figure 1. *ZnO NW ballasted CNT thin films.* SEM micrographs of; **(a)** a dry-transferred[2] CNT film on the flexible and transparent polymer substrate, PET (Scale bar: 2µm). **(b)** a hydrothermally-synthesized ZnO NW coating the dry-transferred (rolled) CNT thin film (Scale bar: 2 µm). **(c)** Emission current showing the ballasting effect of the ZnO NW thin film, particularly in the high-field regime (E > 2 V/µm), and the corresponding Fowler-Nordheim plot **(d)**.

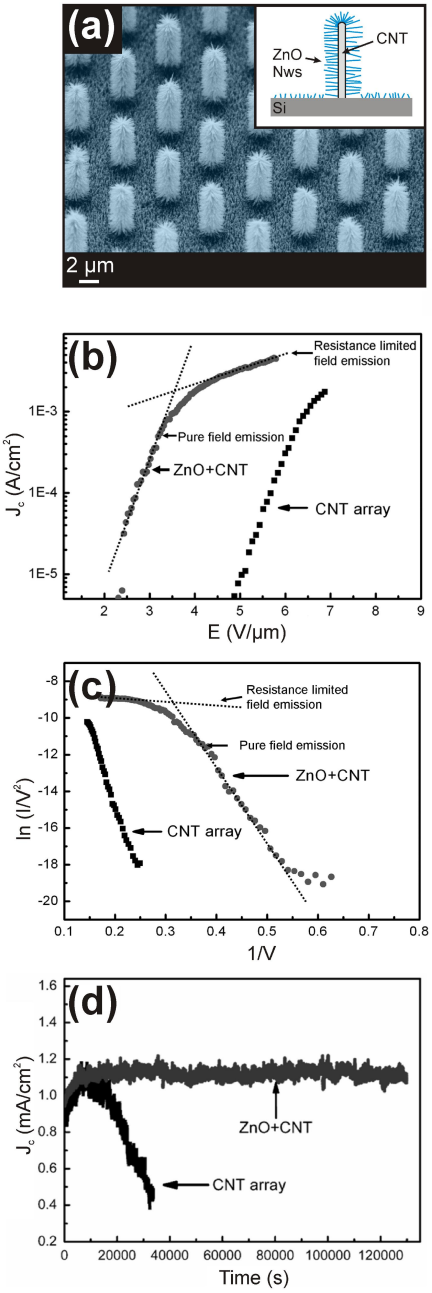

Figure 2. *ZnO NW ballasted CNT arrays.* **(a)** An SEM micrograph of a ZnO NW coated CNT array. *Inset:* Cross section schematic of the emitters (Scale bar: 2 µm). **(b)** Emission current density (J) as a function of the extraction electric field (E). **(c)** Corresponding Fowler-Nordheim plot. **(d)** An accelerated lifetime test showing a distinct increase in emitter longevity as a result of ballast incorporation.[1]

approximately one order of magnitude following ZnO NW deposition. The turn-on electric field (for an emission current of 0.1 µA) of the bare MWCNTs and ZnO NW coated samples were 0.9 V/µm and 1.6 V/µm, respectively. ZnO NWs typically emit at fields of 4-8 V/µm[1, 30-32]. Our earlier studies[1] found, using nominally equivalent hydrothermal ZnO NWs, negligible emission currents for electric fields < 10 V/µm. Thermally synthesized ZnO NWs typically turn-on at lower threshold fields, though rarely less than 3 V/µm[25, 26, 33, 34]. The MWCNT+ZnO NW bi-layer turn-on field is induced by the nanotube support but current-limited by the ZnO NWs. Similar turn-on electric fields from high temperature deposited ZnO nano-multipods on screen printed nanotubes have been reported elsewhere[29].

Figures 2a shows a scanning electron micrograph of an array of vertically aligned CNTs conformally coated with ZnO NWs. **Figures 2b** and **2c** show the field emission performance of these ballasted arrays. These ZnO NWs/CNT

arrays showed a reduction in turn-on field compared to the MWCNT+ZnO NW emitters. The tip-on-tip emitter geometry possibly increased the field enhancement factor, though it has been reasoned in favor of electron tunneling through the MWCNT/ZnO NW interfacial heterojunction[29]. This would, however, suggest that MWCNT thin film and array emitter geometries have equivalent emission characteristics, which is not the case. Another possibility is that the ZnO has a smaller electron affinity (2.1 eV) compared to the nanotube support (4.8 eV), and it therefore has a lower-energy threshold for the electrons escaping from the conduction band into the vacuum. Hence the electrons emit more readily from the nanotube supported ZnO NWs than they would otherwise in a bare metal-supported ZnO NW, for example. Although the presented ZnO NW+MWCNT emitters do indeed turn-on at fields much less than pure ZnO NW emitters (**Figure 2b, c**) the MWCNTs+ZnO NWs do not emit at fields less than the bare MWCNTs, as some studies would suggest[1]. An alternative explanation for the reduced turn-on field of the MWCNT-supported ZnO NWs can be gleaned by considering hot emission. MWCNTs are highly graphitic and conduct with little scattering along their length. They have comparatively low carrier densities, which substantially increases the thermalization time (Metal - 50 fs[35]. CNT - 500 fs[36]). When excited electrons tunnel between adjacent nanotubes excess kinetic energy is gained relative to the local population. Hot electrons accumulate at the uppermost MWCNT at the ZnO NW interfacial Schottky barrier and are injected into the conduction band. The hotter the emission (i.e. the greater the kinetic energy spread of the electrons) the greater the injection depth and the higher the effective field the electrons observe. Thus the emission can be stimulated at lower turn-on fields. The rapid thermalization and high electron densities in more traditional metallic electrodes prevent hot emission, which partly manifests as high turn-on fields. Thus, energetic electrons injected from the MWCNT support into suitably long NW give turn-on fields less than those of the pristine MWCNTs. The proposed model accounts for the lower-than-carbon turn-on fields and rationalizes findings reported elsewhere[1].

Accelerated lifetime measurements ($5x10^{-6}$ mbar), at a current density of 1 mA/cm^2, (**Figure 2d**) revealed that the ZnO NW coated arrays were extremely stable[1], offering lifetimes > 3 times that of their uncoated counterparts. CNTs degrade over time due to surface bound physisorbed species. These lower the local work function, which in semi-metallic field emitters – such as carbon nanotubes and nanofibres – increases the emitted current. Substantial heating can occur which subsequently burns-off the CNT. However, ZnO is a wide band gap semiconductor and any adjustments in the local work function go unnoticed as a result. Hence the observed high degree of stability of ZnO at higher base pressures.

1.2 Ballasted Emission – Silicon on Insulator (SOI)

Though ZnO NW coated CNT arrays offer stable emission their fabrication required the use of prohibitively expensive chemical processes. To obviate this, commercially standardized silicon-on-insulator (SOI) substrates have been used to devise our next generation ballast structures. One such SOI ballasted emitter is shown in **Figure 3a, b**. Here, each CNT emitter is connected in series to a single FET. The emission current increases with the anode-cathode potential difference. The potential drop across the FET channel tends to limit the rise in emission current by reducing the tip-to-anode potential difference.[3] The FET is formed from an undoped Si channel on a 200 nm thick thermally oxidized SiO_2 gate dielectric with asymmetric source-drain contacts.[3] The source is formed from a square W mesh contacting the polycrystalline Si. W is an abundant source of electrons when connected to the negatively biased power supply. The drain contact is formed at the nanotube/catalyst junction which has a contact area of $<10^{14}$ m^2. This drain receives electrons in response to transport through the channel, but cannot source them. The drain is electron deficit. As the current increases, the potential at the drain becomes increasingly positive. Thus the gate-drain potential difference becomes reduces which saturates the emitted current. By electronically controlling the source-drain potential we have demonstrated the ability to controllable limit the emission current density by more than 1 order of magnitude.

Ballasted arrays were fabricated by casting poly(methylmethacrylate) onto SOI substrates (Si<100> /SiO_2 (200 nm)/ Si) patterned by electron beam lithography. A 7 nm Ni CNT-catalyst and a 20 nm ITO diffusion barrier were deposited by direct current magnetron sputtering. The W source was photolithographically defined and deposited in a similar fashion. Nanotubes were grown in a commercially available (Aixtron, Black Magic) plasma enhanced chemical vapor deposition system at 720 ^oC under 200 sccm NH_3 (N5.5) and 50 sccm C_2H_2 (N2.6) at 3 mbar.[37, 38] The nanotubes were

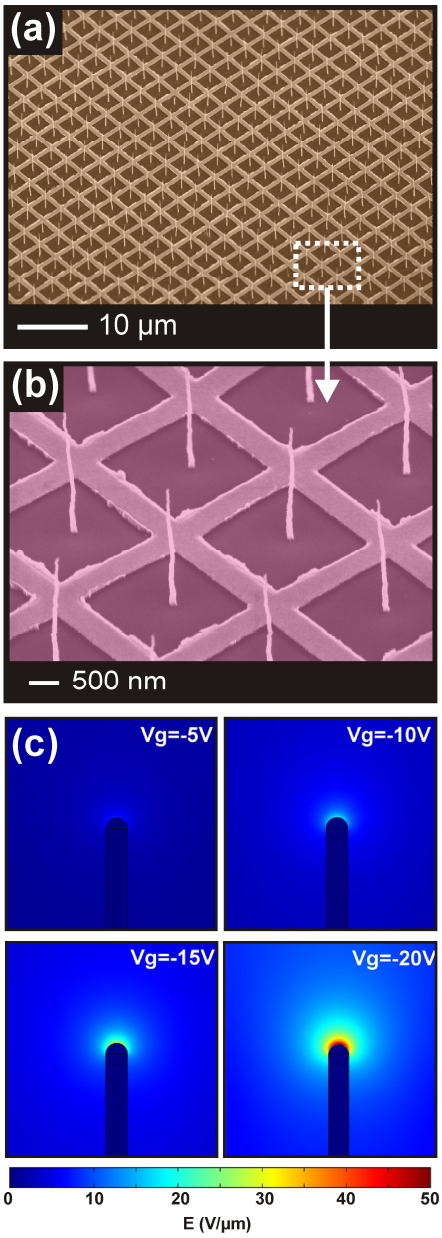

Figure 3. *Silicon-on-Insulator ballasted CNT arrays.* **(a)** A low-magnification SEM micrograph of the fabricated SOI ballasted emitter showing the W bus network (source), the central CNT electron emitter (drain) and the electrically gated Si channel (Scale bar: 10 µm). **(b)** High-magnification image of a few emitters showing the detailed structure of each emitter (Scale bar: 500 nm). **(c)** Variation in the electric field at the CNT tip as a function of (back) gate voltage.[3]

1.25 µm long (±2.4 %) and 80 nm in diameter. EDX and HR-TEM revealed that the Ni catalyst resides at the emitter apex and that the tubes are bamboo-like in crystallinity. W grids were 2.5 µm x 2.5 µm. A single nanotube resides at the center of each square. The total emission area was 0.3 mm x 0.3 mm, with approximately $1.5x10^4$ nanotubes.

Ab-initio simulations (COMSOL v3.4) are given in **Figure 3c**. The cathode is grounded and the anode is biased to 10 V (2 V/µm). The gate electrode is biased at 5, 10, 15, or 20 V and the spatially evolving electric field was monitored. The electric field at the nanotube apex shows a high sensitivity on the gate bias suggesting that an increase in gate voltage of 10 V effectively modifies the local electric field by more than 50 times, which modulates the emission current driven by the anode-cathode potential difference.

Figures 4a and **4b** show the field emission current as a function of anode potential, and the corresponding Fowler-Nordheim plot, respectively. There are three particular regions of interest. For 0-6 V/µm, the noise current dominates. For 6-11 V/µm pure field emission (FN regime) occurs, and for >11 V/µm the transistor-limited emission current is observed. In the FN regime, the driving field is reduced when the gate voltage becomes increasingly negative. At a fixed gate voltage (-20 V) the emission current saturated at 10 mA at an anode voltage of 3.5 kV (14 V/µm), corresponding to a current density of 10 A/cm^2. **Figure 4c** shows an accelerated lifetime measurement. Typical transient responses are shown in **Figure 4d**. The plots are dominated by extremely fast on/off leading and trailing edges, with 90% rise times of < 50 µs. The stability of the ballasted structure showed extremely low emission current fluctuation of 0.68 %, which is, to the best of the authors' knowledge, one of the lowest ever reported. This is attributed to the ballast redistributing the emission current from dominating nanotubes preventing them from burning out, thereby reducing emission current fluctuation and increasing emitter longevity.

Short channel hot electrons evidently enhance the field emission. The large potential drop across the channel causes the electrons accumulating at the drain to become "hot".[39, 40] Hot electrons efficiently propagate through the nanotube and are readily emitted relative to their thermalized counterparts. In conventional field emitters, the distribution in electron energy is largely determined by ambient temperature and axial crystalline defects (electron scatter sites).

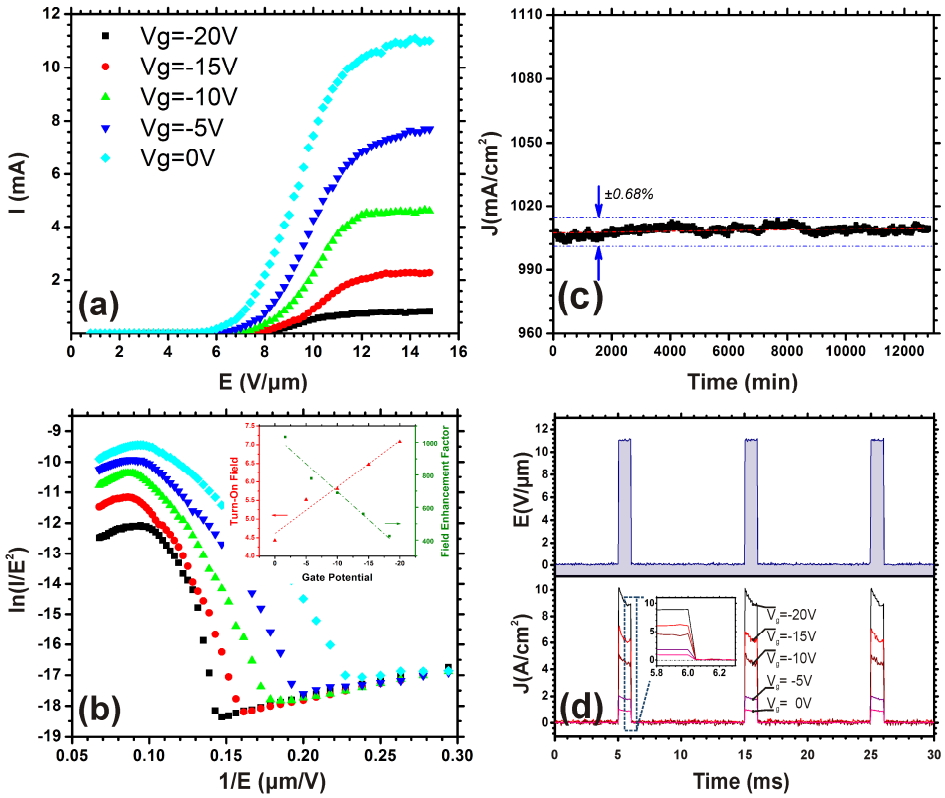

Figure 4. *Emission performance from SOI ballasted CNT arrays.* **(a)** Variation in emission current (I) with extraction field (E) for various gate potentials, **(b)** corresponding Fowler-Nordheim plot. *Inset:* Linear relation in turn-on field (red) and field enhancement factor (green) with gate potential (V^g). **(c)** Accelerated lifetime performance showing highly stable emission (<0.68%). **(d)** Temporal pulsing of the emitter demonstrating a rapid turn on time of < 0.1 ms for various gate potentials ($0V<V_g<20V$).[3]

Multiple scattering ensures thermalization. The emission performance is modified by the injection of hot electrons from the ballast transistor. The electrons are scattered less effectively and arrive at the tip with excess momentum which increases the barriers effective transparency. This increases the transmission probability of the electrons from the Fermi sea at the nanotube apex through the triangular potential barrier and into the vacuum.[41, 42]

In theses SOI ballasted structures the field enhancement factor monotonically decreases with increasingly negative gate potentials. Similarly, the turn-on field (necessary to emit 1 μA) increases linearly with increasingly negative gate potentials (**Inset**, **Figure 4b**). Low gate potentials decrease the channel resistance and therefore increase the carrier energy. This results in a corresponding increase in the injection depth across the Si/nanotube interface. This manifests as a reduction in turn-on fields as these hot electrons propagate deeper into the nanotube before thermalizing, and therefore observe a higher local electric field. The enhanced transmission also leads to an increase in the emission current compared to the unballasted arrays. The increased transmission is most effective in the low-field regime (<6 V/μm), where the carrier transmission is typically very low in conventional arrays[43]. As the electric field increases, the transmission is correspondingly increased, such that the enhancement owing to the hot electrons is diminished.[3]

1.3 Spatial Modulation

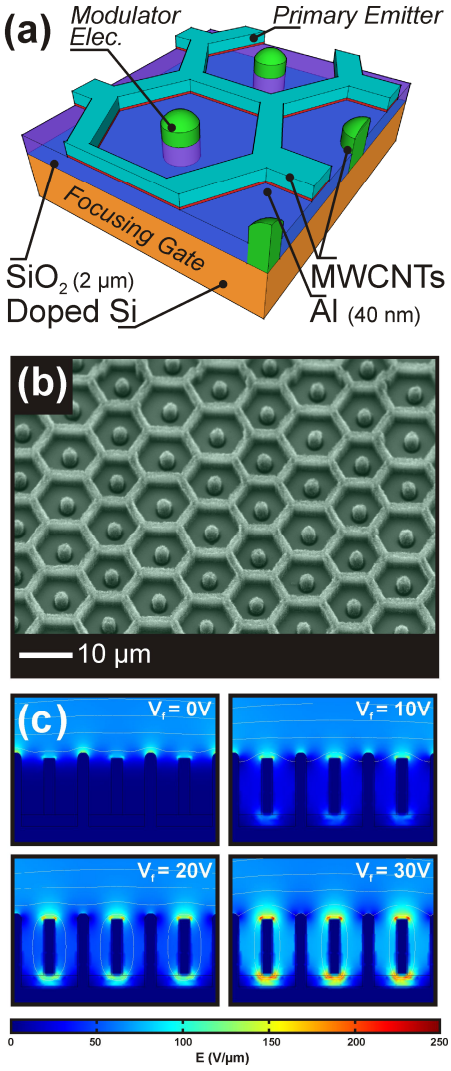

Figure 5. *Focusable triode CNT edge-emitter.* **(a)** Schematic of a beam steerable electron emitter. **(b)** An scanning electron micrograph showing a highly uniform hexagonal edge-emitters with central focusing bundles (Scale bar: 10 μm). **(c)** Simulated equipotentials showing electric field bunching induced by biasing the central focusing bundles.

Large emission currents are important for realizing high brightness FEDs and environmental lighting. High currents are emitted at sharp edges and tips. This is true for in-plane and out-of-plane geometries. We have previously shown that hexagonal honeycomb emitters offer greater current densities compared to full-coverage CNT mats, circular or rectangular patterned CNT emitters; composed of nominally equivalent areal packing densities.[44-46] However, increased spatial control over the emitted electron beam, without the use of multiple gate electrodes, is also desirable and the integration of ways in which to control both the emission current and the electron beams spatial profile will certainly extend the range of applications of such field emitters.

The integrated focussing electrodes, shown in **Figures 5a**, form a triode-like emission structure. The primary emitter is formed from a high current emitting hexagonal array of MWCNTs. Here the central modulating electrode (green) adjusts the electric field distribution associated with the current dominating hexagonal primary emitter. A typical emitter is shown in the scanning electron micrograph of **Figure 5b**. Each pixel is 10 μm and has a 2 μm modulating electrode at its centre formed from a MWCNT bundle. 2-μm holes were defined by electron beam lithography on 200 nm thermally oxidized Si<100> and were through-etched using buffered hydrofluoric acid (49 %). MWCNTs were synthesized by thermal heterogeneous catalysis *via* a bilayer catalyst of natively oxidized Al/Fe (40/1 nm) deposited by direct current magnetron sputtering. MWCNTs deposition took place in a commercially available cold-walled chemical vapor deposition reactor (AIXTRON Ltd., Black Magic) operated at 700 ^{o}C (5 ^{o}C/s) in 192 sccm NH_3 (BOC, N5.5) diluent and 8 sccm C_2H_2 (BOC, N2.6) precursor at 25 mbar. High-resolution transmission electron microscopy, Raman spectroscopy and energy dispersive x-ray (EDX) spectroscopy revealed that the MWCNTs forming the central (modulating) emitters and hexagonal (primary) emitter were nominally equivalent in crystallinity, structure and elemental content. The MWCNTs were 6.0±2.2 (±1 S.D.) nm in diameter and were formed from 4±2 graphene planes. EDX elemental analysis indicated that the emitters were 98.9% C with trace Si (substrate), Al (diffusion barrier) and Fe (catalyst) distributed uniformly throughout their length. Polychromatic (457 nm, 514 nm, 633nm) Raman spectroscopy indicated moderate disorder in crystallinity with a mean D-to-G intensity ratio (I_D/I_G) of 1.35 (±0.13) and I_{2D}/I_G of 0.42 (±0.06).

Figure 5c depicts the evolving cross-section of the electric field for various focusing potentials. Here the voltage between the modulating electrode and primary emitter (hexagon) is increased from 0V to 30V. If the electric field between the primary emitter and modulating emitter becomes significant relative to the anode extraction electric field than large leakage currents are induced, sourced from the primary emitter and sank into the modulating electrode. This

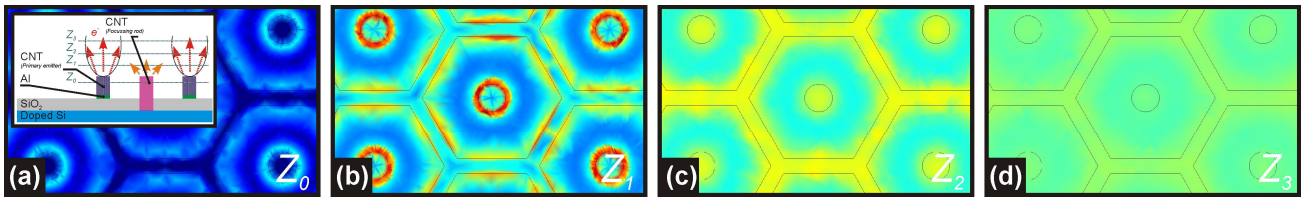

Figure 6. *Electron beam spatial modulation from triode-like CNT edge-emitter*. Variation in the in-plane electric field at various distances from the emitter (intensity arb. u.). Note that even for large Z, where Z >> the height of the emitter perpendicular to the electron extracting electrode, the focusing bundle still imparts a degree of spatial modulation **(d)**.

imposes a strict limit on the range of possible modulator electrode potentials. It is critical that the bulk of the emitted electrons (> 90%) sink into the adjacent anode (i.e. the functional current). **Figure 6** shows the distribution of the in-plane equipotentials at various distances (**a-d**) perpendicular to the emitting surface, as illustrated in the inset of **Figure 6a**. Here the central emitters are biased at -10V and the hexagonal emitters are grounded. By adjusting the potential of the central emitter the distance of the blurring plane (**Figure 6d)** can be controlled. Such routes offer a high speed route and consequent combined control over the emission current and beam spatial modulation.

1.4 Conclusion

Here we have presented our enhanced nano-engineered carbon nanotube electron emitters offering augmented functionality, including; extended stabilities, lifetimes, operation at higher base pressures and beam focusing, through the integration of Si thin film ballasts, ZnO nanowire ballasts and electric field focusing electrodes. Variations in emitter lifetimes as low as 0.7% with on-times of < 1 ms have been measured making such electron emitters promising candidates for next-generation displays, environmental lighting and portable x-rays sources.

ACKNOWLEDGEMENTS

This work was supported by the European Commission through the AXIS project (Grant no. FP7-SME-1-2007) and the Scientific Research Foundation of the Graduate School of Southeast University, China (Grant no. YBJJ0926). M. T. C. thanks St Edmunds College Cambridge University and the Isaac Newton Trust, Trinity College Cambridge, for their generous financial support. D. P. acknowledges support from the national research foundation of Korea and the ministry of education, science and technology (Grant no. R31-2008-000-10029-0).

REFERENCES

[1] Li, C., Zhang, Y., Mann, M., Hiralal, P., Unalan, H. E., Lei, W., Wang, B. P., Chu, D. P., Pribat, D., Amaratunga, G. A. J. and Milne, W. I. (2010). "Stable, self-ballasting field emission from zinc oxide nanowires grown on an array of vertically aligned carbon nanofibers," Appl. Phys. Lett., 96, 143114-143117 (2010).
[2] Cole, M. T., Hiralal, P., Ying, K., Li, C., Zhang, Y., Teo, K. B. K., Ferrari, A. C. and Milne, W. I. (2012). "Dry-transfer of aligned multiwalled carbon nanotubes for flexible transparent thin films," J. Nanomat., 8 (2012).
[3] Li, C., Zhang, Y., Cole, M. T., Shivareddy, S. G., Barnard, J. S., Lei, W., Wang, B., Pribat, D., Amaratunga, G. A. J. and Milne, W. I. (2012). "Hot electron field emission via individually transistor-ballasted carbon nanotube arrays," ACS Nano, 6, 3236-3242 (2012).
[4] Zhang, D., Ryu, K., Liu, X., Polikarpov, E., Ly, J., Tompson, M. E. and Zhou, C. (2006). "Transparent, conductive, and flexible carbon nanotube films and their application in organic light-emitting diodes," Nano Lett., 6, 1880-1886 (2006).

[5] Li, J., Hu, L., Wang, L., Zhou, Y., Gruner, G. and Marks, T. J. (2006). "Organic light-emitting diodes having carbon nanotube anodes," Nano Lett., 6, 2472-2477 (2006).
[6] Choi, J. H., Park, J. H., Moon, J. S., Nam, J. W., Yoo, J. B., Park, C. Y., Lee, C. G. and Choe, D. H. (2006). "Fabrication of carbon nanotube emitter on the flexible substrate," Diam. Relat. Mat., 15, 44-48 (2006).
[7] Rosen, R., Simendinger, W., Debbault, C., Shimoda, H., Fleming, L., Stoner, B. and Zhou, O. (2000). "Application of carbon nanotubes as electrodes in gas discharge tubes," Appl. Phys. Lett., 76, 1668-1670 (2000).
[8] De Jonge, N. and Bonard, J. M. (2004). "Carbon nanotube electron sources and applications," Phil. T. Roy. Soc. A, 362, 2239-2266 (2004).
[9] Milne, W. I., Teo, K. B. K., Amaratunga, G. A. J., Legagneux, P., Gangloff, L., Schnell, J. P., Semet, V., Binh, V. T. and Groening, O. (2004). "Carbon nanotubes as field emission sources," J. Mater. Chem., 14, 933-943 (2004).
[10] Milne, W. I., Teo, K. B. K., Mann, M., Bu, I. Y. Y., Amaratunga, G. A. J., De Jonge, N., Allioux, M., Oostveen, J. T., Legagneux, P., Minoux, E., Gangloff, L., Hudanski, L., Schnell, J. P., Dieumegard, L. D., Peauger, F., Wells, T. and El-Gomati, M. (2006). "Carbon nanotubes as electron sources," Phys. Status Solidi A-Appl. Mat., 203, 1058-1063 (2006).
[11] Hae Jin, K., Jin Joo, C., Jae-Hee, H., Jae Hong, P. and Ji-Beom, Y. (2006). "Design and field emission test of carbon nanotube pasted cathodes for traveling-wave tube applications," IEEE Transactions on Electron Devices, 53, (2006).
[12] Teo, K. B. K., Minoux, E., Hudanski, L., Peauger, F., Schnell, J. P., Gangloff, L., Legagneux, P., Dieumegard, D., Amaratunga, G. A. J. and Milne, W. I. (2005). "Microwave devices - carbon nanotubes as cold cathodes," Nature, 437, 968-968 (2005).
[13] Purcell, S. T., Vincent, P., Journet, C. and Binh, V. T. (2002). "Hot nanotubes: Stable heating of individual multiwall carbon nanotubes to 2000 k induced by the field-emission current," Phys. Rev. Lett., 88, 105502/1-105502/4 (2002).
[14] Baker, F. S., Williams, J. and Osborn, A. R. (1972). "Field-emission from carbon fibers - new electron source," Nature, 239, 96-97 (1972).
[15] Bonard, J. M., Salvetat, J. P., Stockli, T., de Heer, W. A., Forro, L. and Chatelain, A. (1998). "Field emission from single-wall carbon nanotube films," Appl. Phys. Lett., 73, 918-920 (1998).
[16] Chen, T., Wang, L. L., Chen, Y. W., Que, W. X. and Sun, Z. (2007). "Field emission properties of carbon nanotubes film grown on nicr alloy films," Appl. Surf. Sci., 253, 7046-7049 (2007).
[17] Choi, W. B., Jin, Y. W., Kim, H. Y., Lee, S. J., Yun, M. J., Kang, J. H., Choi, Y. S., Park, N. S., Lee, N. S. and Kim, J. M. (2001). "Electrophoresis deposition of carbon nanotubes for triode-type field emission display," Appl. Phys. Lett., 78, 1547-1549 (2001).
[18] Chung, D. S., Park, S. H., Lee, H. W., Choi, J. H., Cha, S. N., Kim, J. W., Jang, J. E., Min, K. W., Cho, S. H., Yoon, M. J., Lee, J. S., Lee, C. K., Yoo, J. H., Kim, J. M., Jung, J. E., Jin, Y. W., Park, Y. J. and You, J. B. (2002). "Carbon nanotube electron emitters with a gated structure using backside exposure processes," Appl. Phys. Lett., 80, 4045-4047 (2002).
[19] De Heer, W. A., Châtelain, A. and Ugarte, D. (1995). "A carbon nanotube field-emission electron source," Science, 270, 1179-1180 (1995).
[20] De Jonge, N., Allioux, M., Doytcheva, M., Kaiser, M., Teo, K. B. K., Lacerda, R. G. and Milne, W. I. (2004). "Characterization of the field emission properties of individual thin carbon nanotubes," Appl. Phys. Lett., 85, 1607-1609 (2004).
[21] Dean, K. A. and Chalamala, B. R. (1999). "The environmental stability of field emission from single-walled carbon nanotubes," Appl. Phys. Lett., 75, 3017-3019 (1999).
[22] Dean, K. A., Chalamala, B. R., Coll, B. F., Xie, Y. W. C. and Jaskie, J. E. (2002). "Carbon nanotube field emission electron sources," New Diam. Front. Carbon Technol., 12, 165-180 (2002).
[23] Teo, K. B. K., Lee, S. B., Chhowalla, M., Semet, V., Binh, V. T., Groening, O., Castignolles, M., Loiseau, A., Pirio, G., Legagneux, P., Pribat, D., Hasko, D. G., Ahmed, H., Amaratunga, G. A. J. and Milne, W. I. (2002). "Plasma enhanced chemical vapour deposition carbon nanotubes/nanofibres - how uniform do they grow?," 3rd International Conference on Trends in Nanotechnology, 204-211 (2002).
[24] Hansung, L., Jihyeon, J., Jeungchoon, G., Ki Buem, K., Naesung, L., Young Chul, C., Hun Soo, K., Jeonyoung, S., Youngdon, P. and Jaiyoung, P. (2009). "Ozone electrical trimming of carbon nanotubes to improve their field-emission lifetime and uniformity," Journal of the Korean Physical Society, 54, (2009).
[25] Wang, X., Zhou, J., Lao, C., Song, J., Xu, N. and Wang, Z. L. (2007). "In-situ field emission of density-controlled zno nanowire arrays," Adv. Mater., 19, 1627-1631 (2007).

[26] Jo, S. H., Lao, J. Y., Ren, Z. F., Farrer, R. A., Baldacchini, T. and Fourkas, J. T. (2003). "Field-emission studies on thin films of zinc oxide nanowires," Appl. Phys. Lett., 83, 4821-4823 (2003).
[27] Greene, L. E., Yuhas, B. D., Law, M., Zitoun, D. and Yang, P. (2006). "Solution-grown zinc oxide nanowires," Inorg. Chem., 45, 7535-7543 (2006).
[28] Anthony, S. P., Lee, J. I. and Kim, J. K. (2007). "Tuning optical band gap of vertically aligned zno nanowire arrays grown by homoepitaxial electrodeposition," Appl. Phys. Lett., 90, 1031071-1031073 (2007).
[29] Yu, K., Zhang, Y. S., Xu, F., Li, Q., Zhu, Z. Q. and Wan, Q. (2006). "Significant improvement of field emission by depositing zinc oxide nanostructures on screen-printed carbon nanotube films," Appl. Phys. Lett., 88, 1531231-1531233 (2006).
[30] Lee, C. J., Lee, T. J., Lyu, S. C., Zhang, Y., Ruh, H. and Lee, H. J. (2002). "Field emission from well-aligned zinc oxide nanowires grown at low temperature," Appl. Phys. Lett., 81, 3648-3650 (2002).
[31] Yang, H. Y., Lau, S. P., Yu, S. F., Huang, L., Tanemura, M., Tanaka, J., Okita, T. and Hng, H. H. (2005). "Field emission from zinc oxide nanoneedles on plastic substrates," Nanotech., 16, 1300-1303 (2005).
[32] Wei, A., Sun, X. W., Xu, C. X., Dong, Z. L., Yu, M. B. and Huang, W. (2006). "Stable field emission from hydrothermally grown zno nanotubes," Appl. Phys. Lett., 88, 2131021-2131023 (2006).
[33] Wang, W., Zhang, G., Yu, L., Bai, X., Zhang, Z. and Zhao, X. (2007). "Field emission properties of zinc oxide nanowires fabricated by thermal evaporation," Physica E, 36, 86-91 (2007).
[34] Li, S. Y., Lin, P., Lee, C. Y. and Tseng, T. Y. (2004). "Field emission and photofluorescent characteristics of zinc oxide nanowires synthesized by a metal catalyzed vapor-liquid-solid process," J. Appl. Phys., 95, 3711-3716 (2004).
[35] Romero, A. H., Garcia, M. E., Valencia, F., Terrones, H., Terrones, M. and Jeschke, H. O. (2005). "Femtosecond laser nanosurgery of defects in carbon nanotubes," Nano Lett., 5, 1361-1365 (2005).
[36] Sun, C. K., Vallée, F., Acioli, L., Ippen, E. P. and Fujimoto, J. G. (1993). "Femtosecond investigation of electron thermalization in gold," Phys. Rev. B, 48, 12365-12368 (1993).
[37] Teo and B., K. (2001). "Plasma enhanced chemical vapor deposited carbon nanotubes for field emission applications," Materials Research Society, (2001).
[38] Chhowalla, M., Teo, K. B. K., Ducati, C., Rupesinghe, N. L., Amaratunga, G. A. J., Ferrari, A. C., Roy, D., Robertson, J. and Milne, W. I. (2001). "Growth process conditions of vertically aligned carbon nanotubes using plasma enhanced chemical vapor deposition," J. Appl. Phys., 90, 5308-5317 (2001).
[39] Forrest, R. D., Burden, A. P., Silva, S. R. P., Cheah, L. K. and Shi, X. (1998). "A study of electron field emission as a function of film thickness from amorphous carbon films," Appl. Phys. Lett., 73, 3784-3786 (1998).
[40] Fitting, H. J., Hingst, T., Schreiber, E. and Geib, E. (1996). "Vacuum emission of hot and ballistic electrons from gaas," J. Vac. Sci. Technol. B, 14, 2087-2089 (1996).
[41] Gomer, R. (1961). "Field emission and field ionization," Harvard Monographs in Applied Sciences, 9, 195 (1961).
[42] Fowler, R. H. and Nordheim, L. (1928). "Electron emission in intense electric fields," Proc. R. soc. Lond. Ser. A-Contain. Pap. Math. Phys. Character, 119, 173-181 (1928).
[43] Teo, K. B. K., Chhowalla, M., Amaratunga, G. A. J., Milne, W. I., Pirio, G., Legagneux, P., Wyczisk, F., Pribat, D. and Hasko, D. G. (2002). "Field emission from dense, sparse, and patterned arrays of carbon nanofibers," Appl. Phys. Lett., 80, 2011-2013 (2002).
[44] Nguyen Tuan, H., Ken Ha, K., Soonil, L., Phan Ngoc, M., Ngo Thi Thanh, T. and Phan Hong, K. (2009). "Comparison of field-electron emission from different carbon nanotube array structures," Journal of Vacuum Science & Technology B (Microelectronics and Nanometer Structures), 27, (2009).
[45] Liu, P., Liu, L., Wei, Y., Sheng, L. and Fan, S. (2006). "Enhanced field emission from imprinted carbon nanotube arrays," Appl. Phys. Lett., 89, (2006).
[46] Killian, J. L., Zuckerman, N. B., Niemann, D. L., Ribaya, B. P., Rahman, M., Espinosa, R., Meyyappan, M. and Nguyen, C. V. (2008). "Field emission properties of carbon nanotube pillar arrays," J. Appl. Phys., 103, (2008).